Annu. Rev. Fluid Mech. 1999. 31:239–72

FLOW CONTROL WITH NONCIRCULAR JETS[1]

E. J. Gutmark
Mechanical Engineering Department, Louisiana State University, Baton Rouge, Louisiana 70803-6413; e-mail: gutmark@me.lsu.edu

F. F. Grinstein
Laboratory for Computational Physics and Fluid Dynamics, Code 6410, Naval Research Laboratory, Washington, DC 20375-5344;
e-mail: grinstei@lcp.nrl.navy.mil

KEY WORDS: vortices, mixing, combustion, entrainment

ABSTRACT

Noncircular jets have been the topic of extensive research in the last fifteen years. These jets were identified as an efficient technique of passive flow control that allows significant improvements of performance in various practical systems at a relatively low cost because noncircular jets rely solely on changes in the geometry of the nozzle. The applications of noncircular jets discussed in this review include improved large- and small-scale mixing in low- and high-speed flows, and enhanced combustor performance, by improving combustion efficiency, reducing combustion instabilities and undesired emissions. Additional applications include noise suppression, heat transfer, and thrust vector control (TVC).

The flow patterns associated with noncircular jets involve mechanisms of vortex evolution and interaction, flow instabilities, and fine-scale turbulence augmentation. Stability theory identified the effects of initial momentum thickness distribution, aspect ratio, and radius of curvature on the initial flow evolution. Experiments revealed complex vortex evolution and interaction related to self-induction and interaction between azimuthal and axial vortices, which lead to axis switching in the mean flow field. Numerical simulations described the details and clarified mechanisms of vorticity dynamics and effects of heat release and reaction on noncircular jet behavior.

The research on noncircular jets has also led to technology transfer. A topic that started as an academic curiosity—an interesting flow phenomenon—subsequently has had various industrial applications. The investigations reviewed include experimental, theoretical, numerical, and technological aspects of the subject.

INTRODUCTION AND BACKGROUND

The mixing process in jet shear layers involves bulk mixing driven by large-scale coherent structures, and smaller-scale mixing dominated by turbulent velocity fluctuations. Large-scale coherent structures (CS), characterized by organized vorticity distributions, are intrinsic features of the high Reynolds number (Re) mixing layer (Brown & Roshko 1974). Control of jet development in practical applications is strongly dependent on understanding the dynamics and topology of CS, in particular, how jet properties can be affected by control of the formation, interaction, merging, and breakdown of CS.

Formation of circular, azimuthally coherent vortex rings and their sequential merging dominate the shear-layer growth and entrainment in axisymmetric jet configurations at moderately high Re (Crow & Champagne 1971). At a short distance downstream of the jet exit, three-dimensionality becomes the crucial feature of the jet structure, and the streamwise vorticity has the dominant role in entraining fluid from the surroundings (Liepmann & Gharib 1992). Self-induction, vortex stretching, and reconnection become the dominant fluid-dynamical processes involved (Hussain 1986). Azimuthal nonuniformities at the jet exit add complexity to the evolution of the jet shear layer; the three-dimensional development of the jet is particularly sensitive to initial conditions determined, for example, by the nozzle geometry or by upstream disturbances. In noncircular jets, deformation dynamics of asymmetric vortices play an important role in the jet evolution. Asymmetric jets are naturally more unstable than their axisymmetric counterparts (Michalke 1971). Amplification of high-order instability modes rather than the axisymmetric mode that dominates the near-field region of a circular jet, brings about complex vortex topologies. Elongated jets, for example, tend to exhibit lateral flapping motion along their minor axes (Crighton 1973).

Substantial efforts have been devoted to investigating the properties of jets emerging from noncircular nozzles. Laboratory studies using elliptic nozzles (Ho & Gutmark 1987, Husain & Hussain 1983, Hussain & Husain 1989) and nozzles with corners, e.g. rectangular, triangular, star-shaped (Gutmark et al 1989a, Toyoda & Hussain 1989, Quinn 1992), have observed that as the jet spreads, its cross-section can regularly evolve through shapes similar to those of the jet nozzle but with axes successively rotated at angles characteristic of the

jet geometry, denoted as the axis-switching phenomenon. This main underlying mechanism for the enhanced entrainment properties of noncircular jets, relative to comparable circular jets, results from self-induced Biot-Savart deformation of vortex rings with non-uniform azimuthal curvature and interaction between azimuthal and streamwise vorticity. Due to Biot-Savart self-induction, portions of the vortex with small radius of curvature, such as the major axis section of elliptic rings or the vertices in square or triangular rings, will move downstream faster than the rest, leading to their deformation. As the vortex convects downstream, the deformations yield a complex topology, which results in redistribution of energy between azimuthal and streamwise vortices whose subsequent interaction increases the small-scale content of the jet.

In supersonic planar, axisymmetric, and noncircular shear layers, the effect of compressibility on mixing becomes important and adds to the effects of velocity and density gradients and azimuthal distribution. The convective Mach number (Mc) (Bogdanoff 1982, Roshko & Papamoschou 1986) quantifies the compressibility effect. This parameter is defined as the relative convection speed of the large-scale structures in the shear layer to one of the free streams, normalized by the speed of sound of the latter. The spreading rate of a plane shear layer drops sharply to about 20% of the incompressible spreading rate as $\mathrm{Mc} > 0.6$. Supersonic shear layers exhibit augmented three-dimensional vortical structure due to preferential amplification of high modes of instability. Therefore, noncircular jets that are inherently dominated by high azimuthally unstable modes are particularly suitable for enhancing mixing in supersonic flows.

Shear-flow control methods seek to enhance the three-dimensionality of the flow, and thus entrainment and mixing, by manipulating the natural development of CS and their breakdown into turbulence. Passive mixing-control strategies are based on geometrical modifications of the jet nozzle, which alter the flow development downstream of the nozzle relative to a conventional circular nozzle. Interest in noncircular jets was driven primarily by the potential to obtain enhanced mixing between jet flow and surroundings. Elliptic and rectangular jets were shown to have entrainment rates significantly larger than those of circular or two-dimensional jets due to vortex self-induction effects (Ho & Gutmark 1987, Austin 1992). Enhanced mixing was observed in both subsonic and supersonic jets. Large-scale CS in natural planar shear layers (Bernal & Roshko 1986) and axisymmetric jets (Liepmann & Gharib 1992) were altered and deformed by interaction with secondary streamwise vortices, with streamwise-vortex generation locations dependent on upstream disturbances. The interaction between azimuthal and streamwise vortices constitutes an important process, which can be used as an independent method of mixing enhancement in circular, plane jets, or in conjunction with noncircular jet geometries to achieve additional enhanced mixing. Controlled streamwise vortex generation can be achieved

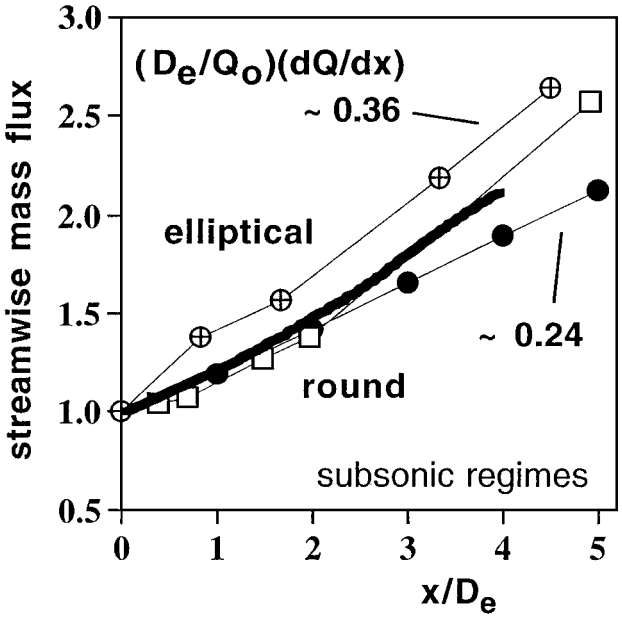

Figure 1 Near-field entrainment measurements in noncircular jets. From experiments: (*crossed circles*) elliptic jets, (Ho & Gutmark 1987), (*squares*) square jets (Grinstein et al 1995), (*dark circles*) round jets (Zaman 1986). From computational studies (simulations): (*bold line*) square jets. (Grinstein et al 1995)

using different azimuthal perturbation methods, including corrugated, lobed, or indented nozzle edges, vortex generators, or other nozzle shaping concepts.

In Figures 1 and 2, measurements of the subsonic jet entrainment for various low aspect-ratio noncircular geometries are compared with typical axisymmetric jet data, based on evaluations of the normalized streamwise mass flux Q/Q_o. Significant near-field entrainment augmentation is evident when using noncircular geometries (Figure 1), e.g. entrainment rates $D_e/Q_o(dQ/dx)$ about 50% larger for $2D_e < x < 4D_e$, where D_e is the jet circular-equivalent diameter—defined as the diameter of an axisymmetric jet having the same cross-sectional area at the jet exit. In the far field (Figure 2), the entrainment rates of noncircular jets asymptotically approach the round jet value, reflecting the jet's tendency to develop into an axisymmetric structure. However, because high far-field values of Q/Q_o are due to high near-field entrainment rates, actual jet initial conditions (e.g. nozzle geometry, presence of vortex generators) leave a clear imprint on the far-field jet behavior by affecting the near-field jet stability characteristics and vortex dynamics controlling spreading and deformation of the transverse jet cross-section.

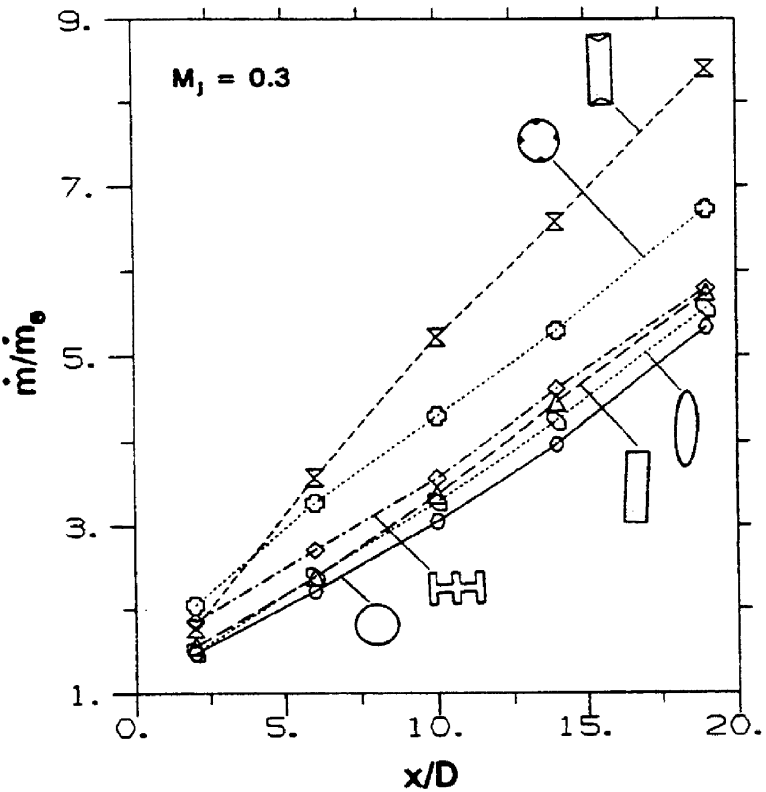

Figure 2 Far-field entrainment measurements in noncircular jets, from experimental studies. (Zaman 1996a)

In the second section of this paper, the laboratory investigations using noncircular jet configurations are reviewed, including the use of various geometrical nozzle modifications grouped into three categories: (*a*) elongated geometries, such as those of elliptic and rectangular jets, (*b*) jets issued from nozzles with corners, such as square and triangular configurations, and (*c*) jets issued from nozzles incorporating axial-vorticity generators; the second section concludes with a discussion summarizing the noncircular jet research in reacting and supersonic regimes. The third section of this paper synthesizes the physical mechanisms that are common to the different jet configurations; these include stability analysis, effects of initial conditions on axis switching, vortex dynamics, interaction between azimuthal and longitudinal vortices, and effects of aspect ratio. Finally, the various applications of these jets are discussed.

NONCIRCULAR JETS—LABORATORY EXPERIMENTS

Isothermal Flows

ASPECT RATIO EFFECTS—ELLIPTIC AND RECTANGULAR JETS Elliptic and rectangular jets were investigated extensively because of their increased entrainment and enhanced mixing properties (Sfeir 1975, 1976, 1979; Husain & Hussain 1983; Ho & Gutmark 1987; Quinn 1989; Austin 1992). The large-scale mixing of the elliptic jet was found to be substantially larger relative to the circular jet due to axis switching associated with the self-deformation of elliptic vortices (Dhanak & Debernardinis 1981). Ho & Gutmark (1987) reported enhancement of small-scale mixing due to the amplification of high azimuthal instability modes.

Axis switching results from faster growth rate of the jet's shear layers in the minor axis plane (plane parallel to the elliptic minor axis) compared to those in the major axis plane (Figures 3 and 4). These differential growth rates result in a crossover point at a certain downstream distance from the nozzle where the jet's dimensions at the two axes are equal. In general, the growth rate of the jet depends on many parameters, such as Reynolds number, initial turbulence level and spectral content emanating from upstream disturbances, velocity and temperature ratio, nozzle geometry and aspect-ratio, and initial circumferential shear-layer thickness distribution. Quinn (1989) compared his measurements of an elliptic jet issuing through a 5:1 elliptic orifice at $\mathrm{Re} = 2.08 \times 10^5$ with 2:1 elliptic jets emanating from a contoured nozzle at a similar $\mathrm{Re} = 1 \times 10^5$ (Husain & Hussain 1983, Ho & Gutmark 1987). The crossover location varied from 3 to 7 jet equivalent diameters. All jets had an initial turbulence level of 0.4 to 0.5%. The difference between Quinn's jet and the other two were attributed to differences in nozzle geometry, i.e. orifice versus contoured nozzle, which yield a different distribution of the initial shear-layer thickness distribution. The jets with nearly uniform initial shear layer studied by Husain & Hussain (1983), compared with a jet having 26% circumferential variation in the case of Ho & Gutmark (1987), also resulted in different entrainment rates. Austin (1992) showed that the location of the first axis switching moved downstream with increased mean exit velocity and inversely with exit temperature (density ratio). This latter trend was confirmed by linear stability calculations, which showed decreased growth rate of disturbances with the addition of heat release (Huang et al 1994). The higher mixing rate of the elliptic jet resulted in a reduction of the potential core length to three to four equivalent jet diameters compared to five diameters for the circular jet.

The small-scale mixing was coupled with the evolution of the large-scale vortices and was enhanced as a result of high azimuthal instability modes amplified in noncircular configurations. The mixing enhancement was found to be

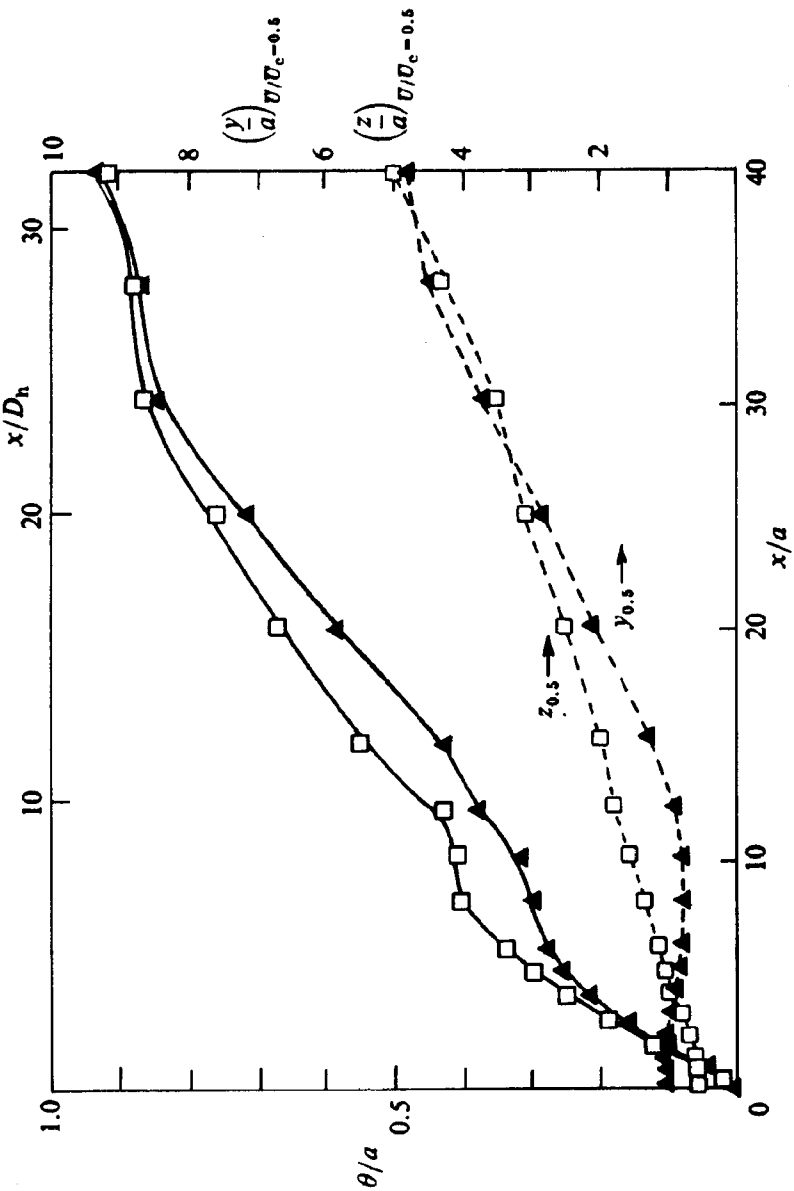

Figure 3 (y/a and z/a) Jet half-widths and (θa) momentum thickness as a function of normalized downstream distance (x/a, a is half major axis), of a 2:1 elliptic jet at the major (*triangles*) and minor (*squares*) axis planes. (Ho & Gutmark 1987)

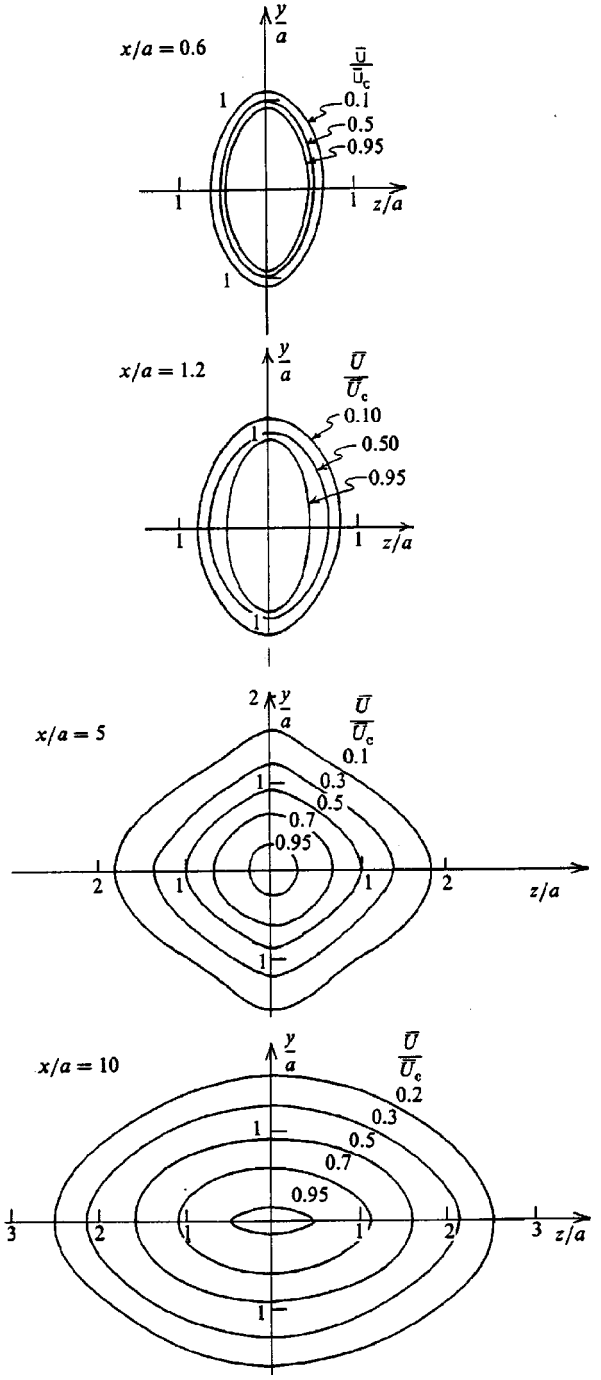
x/a = 0.6
y/a
Ū/U_c
0.1
0.5
0.95
z/a
x/a = 1.2
0.10
0.50
0.95
x/a = 5
0.1
0.3
0.5
0.7
0.95
x/a = 10
0.2
0.3
0.5
0.7
0.95

effective for high Reynolds numbers and for reacting flows (Schadow et al 1987b). In circular jets, the main mechanism leading to the shear-layer growth and formation of small-scale structures is the vortex interaction and merging process (Ho & Huerre 1984). In contrast, in the case of the elliptic jet, the dynamics of vortex self-induction turns out to be more important than the vortex merging process. Austin (1992) measured nearly equal mass entrainment values for both forced and natural elliptic jets, demonstrating this fact. He also showed that a heated or low-speed ($M = 0.1$) elliptic jet entrains up to 30% more mass than a cold or a higher-speed ($M = 0.25$) elliptic jet as the axis switching moved closer to the nozzle. His measurements confirmed that production of small-scale structures is related to the vortex deformation process and showed that the small scales are concentrated within the large-scale vortex cores. Tsuchiya et al (1986) showed that the axial turbulence component along the jet's axis increases faster for large aspect ratio in the orifice elliptic jet. In all elliptic jets studied, i.e. orifice, contoured, and pipe nozzles, the turbulence growth rate reduced with Reynolds number; however, the effect was minimal in pipe jets.

Rectangular jets combine the aspect ratio (AR) features of an elliptic jet with the corner (vertex) features of square jets. Nozzle exit shape, AR, initial turbulence level, and Re affect the development of the jet. The spreading rate of the rectangular jet is typically higher at the wide section than at the narrow side. This results in axis switching similar to that of an elliptic jet. Detailed investigation into the vortex dynamics of a confined 2:1 rectangular jet revealed similar features to those of the elliptic jet (Hertzberg & Ho 1995). The distance of the crossover location from the nozzle was found to be directly proportional to the nozzle aspect-ratio (Figure 5). Tsuchiya et al (1986) presented measurements of four rectangular orifice jets with AR varying from 1 to 5. The crossover location varied from less than 1h (width of narrow dimension) to nearly 10h, respectively. The crossover location of the 2:1 contoured rectangular nozzle was slightly closer to the nozzle. Quinn (1992b) reported a similar trend in an investigation on the effect of AR on the development of orifice rectangular jets. In his measurements, the crossover location varied from 1 to 12 equivalent diameters for AR between 1 to 20. In both investigations, the jet growth rate at the minor exit plane was high; the jet width at the major axis plane was initially reduced due to the vena contracta effect. Following axis switching, the major-axis growth rate became higher than at the minor axis, resulting in a second axis switching farther downstream. The second crossover location was much less sensitive to the original AR of the nozzle.

←

Figure 4 Velocity contours along the elliptic jet axis exhibiting axis switching. (Ho & Gutmark 1987)

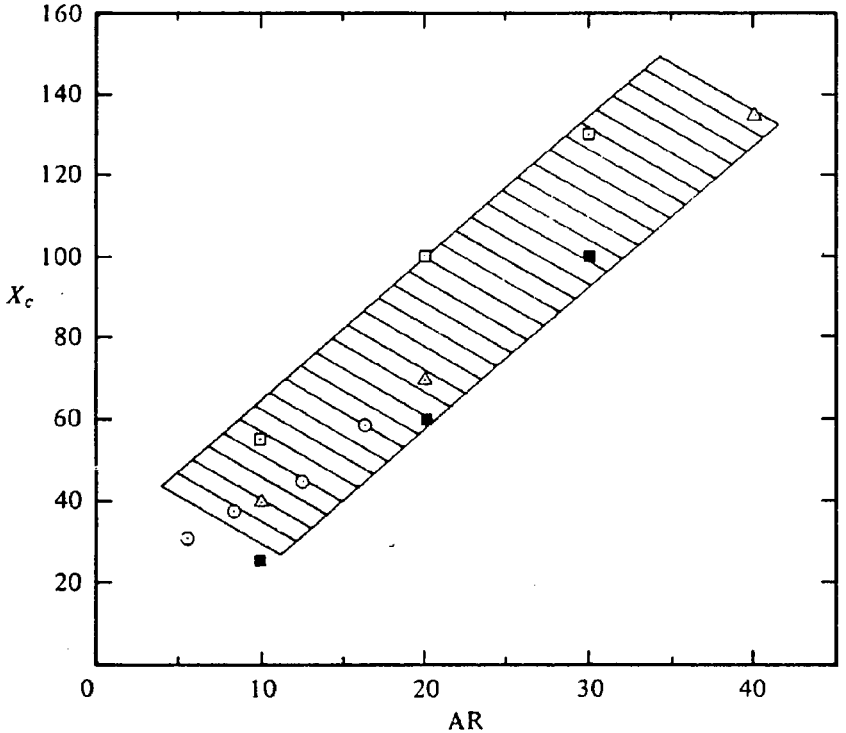

Figure 5 Variation of axis-switching location in a rectangular jet with nozzle aspect-ratio (*AR*). (*open squares*), (*dark squares*) (Sfein 1976); (*circles*) (Krothapalli 1981); (*triangles*) (Sforza 1966)

The instability modes of a 4:1 rectangular jet were studied by Shih et al (1992). In the very low subsonic range the dominant instability mode was symmetric. For all higher jet velocities, the antisymmetric mode was most amplified, except in the range of $0.6 < M < 0.85$ in which both symmetric and antisymmetric modes coexisted with continuous switching between them. The preferred mode of the jet varied proportionally to the square root of the exit Re.

NOZZLES WITH CORNERS—SQUARE AND TRIANGULAR JETS Early investigations of nozzles with corners concentrated on the mean flow field of triangular and square jets (Sforza et al 1966, Trentacoste & Sforza 1967). Later studies of jets emerging from noncircular nozzles with corners showed that the introduction of sharp corners in the nozzle can increase significantly the fine-scale turbulence at the corners relative to the flat segments of the nozzle (Schadow et al 1988, Toyoda & Hussain 1989) and enhance mass entrainment (Vandsburger &

Ding 1995). Even in the case of the acoustically forced triangular shear layer, only small-scale turbulent flow emanated from the corners, whereas highly coherent structures were generated at the flat sides. In some cases, the small-scale turbulence was produced by three-dimensional flow, which was formed at the corner regions inside the nozzle (Su & Friedrich 1994).

The evolution of square and triangular jets is characterized by differential shear-layer growth rates at the flat and vertex sections. This difference in spreading rate may lead to axis switching, or rotation of the jet geometry in the downstream direction. The production of small-scale turbulence is also different in the various circumferential sections. This behavior depends on the initial conditions at the jet exit that subsequently affect the vortex dynamics. Grinstein et al (1995) discussed the role of initial conditions and other parameters that affect the near field of a subsonic square jet. They examined effects of initial conditions such as ratio of initial-momentum-thickness to circular-equivalent-diameter, turbulence level, azimuthal momentum thickness distribution, and Reynolds number effect on the jet shear-layer growth pattern. Axis switching was shown to be related to vortex deformation dynamics, which in turn was enhanced at a low turbulence level and thin initial shear layer. The dependence on Reynolds number and jet Mach number (M) was very weak. High azimuthal coherence level and small shear-layer thickness to jet diameter ratio were crucial for the initiation of strong vortex deformation and self-induction process. When these conditions were not satisfied—as in a pipe square jet—axis switching was not observed (Figure 6), and lower entrainment rates were obtained. Vortex deformation in the square jet is initiated at the corners by downstream bending of the corner sections due to the small local radius of curvature. Stretching of the bent vortex by the shear stresses produces small-scale streamwise vortices at the corners. This process, which is unique to jets flowing from nozzles with corners, results in the initial axis switching and amplification of small-scale turbulence at the vertices. The ensuing complex vortex interaction between azimuthal and streamwise structures makes the role of vortex ring deformation dynamics limited in the subsequent occurrence of axis switching (discussed further below).

AXIAL VORTICITY GENERATORS IN JETS An alternative approach to passive near-field entrainment augmentation using noncircular nozzles consists of breaking the axisymmetry of a circular jet and promoting streamwise vorticity production at the jet exit. In early studies by Bradbury & Khadem (1975), axial vorticity was introduced by placing tabs at the jet exit such that they protruded into the flow (typically with an area blockage of 1–2% per tab). The concept, originally tested in subsonic jets, showed that the most effective configuration consisting of two tabs could reduce the potential core length and increase the decay of the centerline velocity. In later investigations, streamwise

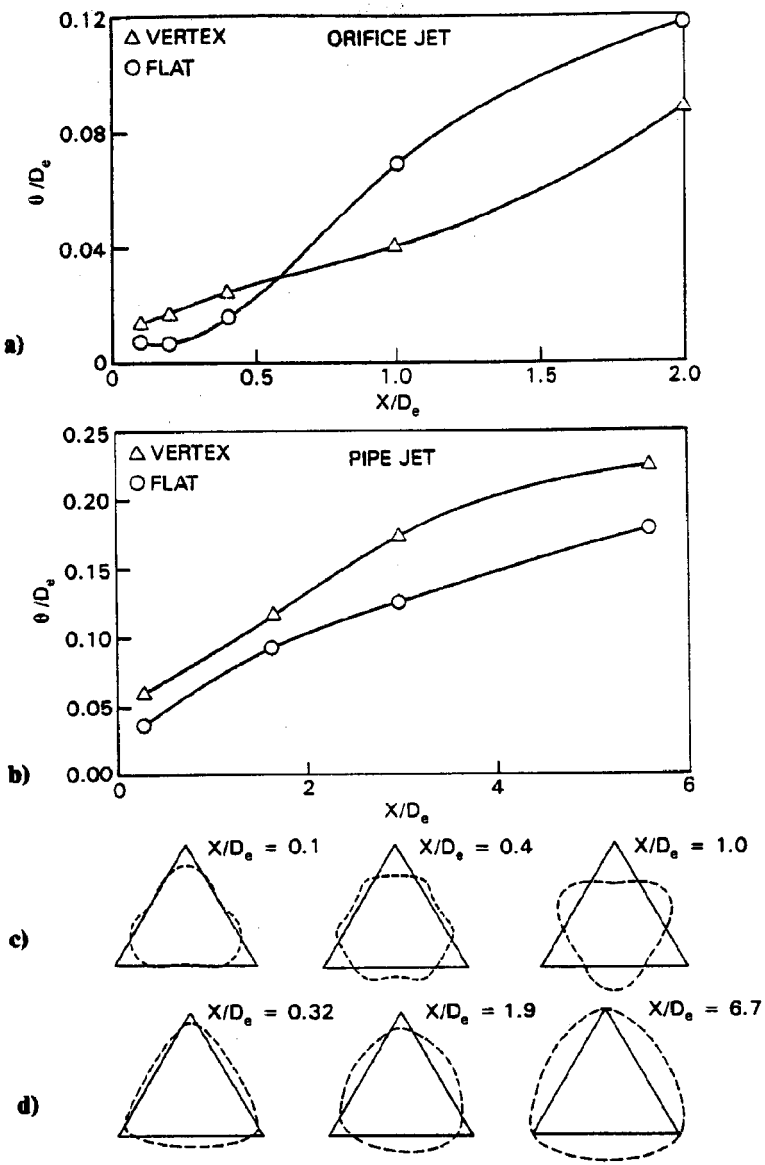

Figure 6 Variation of momentum thickness with axial distance at the vertex and flat sides of the triangular jet: (*a*) orifice jet, (*b*) pipe jet. Corresponding evolution of the jet cross-sections along the axis: (*c*) orifice jet, (*d*) pipe jet. (Koshigoe et al 1989)

Figure 7 Dynamics of azimuthally excited round jets with annular fuel injection (Grinstein et al. 1996).

vorticity generation at the jet exit was promoted by enforcing azimuthal excitation through suitable vortex generators or tabs at the edge of the nozzle (Ahuja & Brown 1989, Zaman 1991), "entrainment manipulators" upstream of the jet exit (Monkewitz & Pfizenmaier 1991), or by using indented or corrugated nozzles (Lasheras et al 1991).

Grinstein et al (1996) studied azimuthally excited round air jets emerging into quiescent air background, with special focus on investigating the near-field jet entrainment and associated combustion dynamics of fuel injected along a thin, annular region at the rim of the nozzle. The reaction zones in the jet were visualized using OH Planar-Laser-Induced-Fluorescence (PLIF) diagnostics. Both axisymmetric and azimuthal modes of the jet were excited to stabilize its spatial structure. Three-dimensional visualization of the reacting laboratory jet, reconstructed from multiple two-dimensional images acquired at constant phase angle, could yield only the structure of the reaction zones that were the end result of complex three-dimensional processes. Time-dependent numerical simulations were used to gain insight into the dynamics and topology of the fluid-dynamical processes underlying the observed flame structure. Flow visualizations of experimental and computational jets were found to strongly resemble each other (Figure 7*a*; see color section), revealing tight coupling between ring and braid (rib) vortices (Figure 7*b*). As a result of the streamwise vorticity introduced at the jet exit, the transverse section of the axisymmetric jet shear layer deformed into a pentagonal shape, the imprint of which was also imposed on the vortex rings. The self-deformation of the vortex rings due to rapid change in azimuthal curvature at corner regions of the pentagon led to a subsequent 36-deg axis rotation of the jet cross-section, similar to the behavior described earlier in noncircular jets. The vorticity dynamics and ensuing mixing processes determine the regions of combustion within the flame and thus the overall heat release pattern (Figure 7*c*). The jet vorticity evolution was found to be dominated by the dynamics of vortex-ring self-deformation induced by the azimuthal excitation imposed at the jet exit, the dynamics of rib vortices forming in the braid regions between undulating vortex rings, and strong interactions between ring and rib vortices—consistent with the earlier reported studies of azimuthally excited round jets by Lasheras et al (1991) and Martin & Meiburg (1991). Vortex interactions and azimuthal instabilities in azimuthally excited round jets lead to lateral flow ejections in hot jets (Monkewitz & Pfizenmaier 1991) and axially forced cold jets (Lasheras et al 1991); depending on the amplitude and frequency of the axial forcing, several distinct side-ejection vorticity modes are observed (Figure 8).

The concept of axial vortex mixing was considered for turbofan engines for which the lobed mixer was proposed (Paterson 1984). This design provided larger contact interface between the two mixing flows and generated large-scale

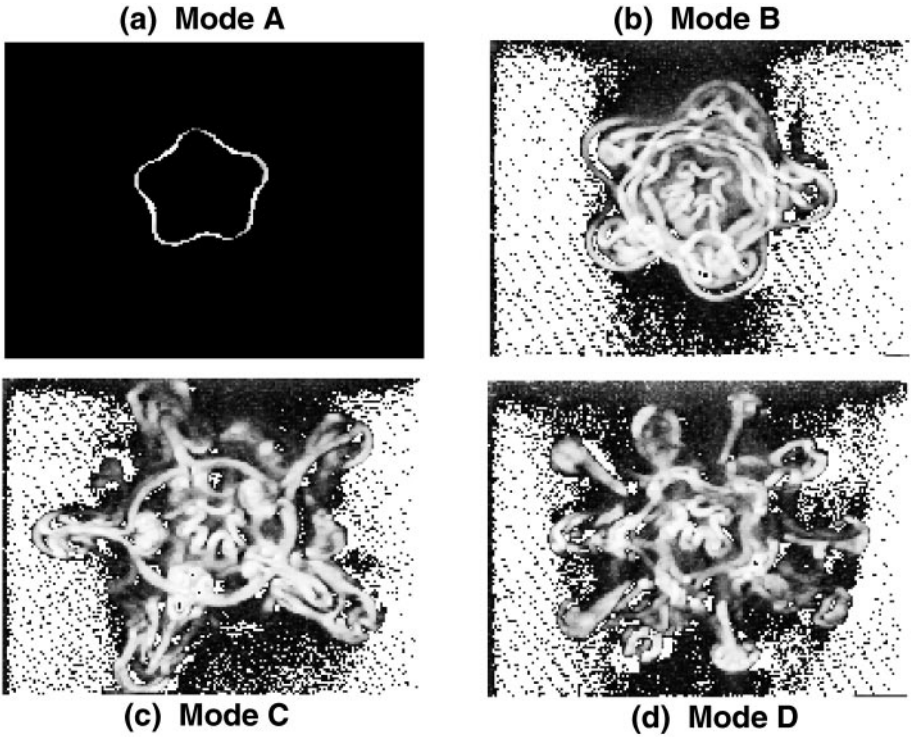

Figure 8 Cross-stream TiO_2 flow-visualization at x/D = 3 of five-lobed, axially forced laminar jets showing distinct modes of lateral ejections. (Lasheras & Prestridge 1997)

axial vortices that enhanced mixing and interacted with the spanwise vortices shed from the convoluted splitter-plate. Based on this concept, two-dimensional lobed nozzles were tested in low subsonic flow and compared to rectangular and circular jets. The enhanced mixing of the lobed nozzle resulted in reduction of the jet potential core length by 2–3 times relative to the rectangular jet and 4–6 times relative to the circular jet (Liu & Wu 1995).

An alternative geometry proposed to generate axial vorticity in an elliptic jet was the tapered slot nozzle. The nozzle consisted of a conical contraction region, which led into the slotted outlet. Gutmark & Schadow (1987) described the basic flow characteristics of this jet. The jet shear-layer growth pattern was different from that of the elliptic jet. The jet spread in the major axis side was larger than in the minor axis side. Consequently, axis switching was not observed in this jet. The growth rate of the turbulence level in the core region, as well as in the jet's circumference, was higher than in the circular and elliptic

jets. The increased turbulence production was related to the axial vorticity component generated by the nozzle geometry.

Reacting Flows

Noncircular injectors such as elliptic, triangular, and square nozzles were used to improve combustion processes by augmenting heat release, reducing emissions, and improving flame stability. Some examples for these applications are reviewed in this section.

Schadow et al (1987) conducted tests in a hot jet within a gas-generator ramjet configuration, in which a fuel-rich plume exhausted into a co-flowing air and afterburned in a secondary combustion chamber. The temperatures obtained in the secondary chamber, when the plume issued from an elliptic nozzle, were increased by more than 20% relative to a circular injector. The highest overall heat release was obtained using a 3:1 elliptic injector. Comparison between circular and elliptical air inlets in dump combustor experiments yielded similar results (Schadow et al 1987b). The temperature increase near the combustor centerline was more than doubled using an elliptic inlet relative to a circular one, due to the enhanced fuel mixing produced by the elongated nozzle. Gollahalli et al (1992) tested diffusion flames of gas jets issued from elliptic nozzles and compared them to circular nozzles. They reported high heat release and lower soot concentration of the elliptic flame compared to the circular flame. NOx was reduced by 20% when an elliptic Ventury inlet was used in an inshot burner of a gas furnace due to increased air entrainment (Kolluri et al 1996).

Gutmark et al (1989a) investigated acoustically forced triangular flames. Large-scale coherent structures at the flat sides and small-scale flamelets at the corners characterized the flame. The differences between the flat sides and the corner sections were more pronounced for small, acute corner angles. The circumferential variation of the jet's spreading rate led to changes in the cross-sectional geometry of the flame along its axis. Axis switching was observed for equilateral triangular and square flames but not for an isosceles triangular flame with a 30-deg vertex angle. Combustion systems with triangular and square jets can benefit from this combination of large- and small-scale mixing. The large-scale vortices promote fast bulk mixing between fuel and air, while small-scale turbulence accelerates the combustion rate by enhancing mixing at the molecular level. Another advantage of nozzles with corners is related to combustion instabilities. Combustion instabilities can be excited when periodic heat release associated with large-scale vortex mixing interacts with resonance acoustic modes in the combustion chamber. Excitation of combustion instability can be avoided when fuel is injected into the fine-scale turbulence at the corner regions rather than into the large-scale vortices at the flat sections. At the

same time, the large-scale mixing at the flat sides entrains air into a diffusion flame, or hot combustion products into a premixed flame, needed to sustain the combustion process. The early initiation of combustion at the corners, where the ambient air entrainment is low, increases the local temperature of the combustion products, thus leading to efficient and stable combustion. The unique shear-flow development of triangular jets was used to suppress pressure oscillations in a coaxial dump combustor, simulating a ramjet engine (Schadow et al 1990). Pressure oscillations as high as 37% of the mean pressure were measured in a combustor with a circular inlet duct, or when fuel was injected into the triangle's flat sides. Injection of fuel into the corner sections reduced the amplitude of the pressure oscillations to below 10% of the mean pressure. The pressure amplitude was dependent on the direction of fuel injection and on the extent of fuel penetration into the air stream. The dump combustor with a triangular inlet achieved higher combustion efficiency and operated in a lower flammability limit. Similar reduction of combustion instability was obtained in a dump combustor with variable length-to-diameter ratio (Whitelaw et al 1988).

Supersonic Flows

The development of the High Speed Civil Transport (HSCT) and other high-speed airplanes prompted interest in achieving rapid mixing of supersonic flows for combustion purposes and noise reduction while minimizing the thrust loss penalty associated with mixing-enhancement techniques. In this context, several noncircular geometries were considered as a possible solution.

The mixing characteristics of noncircular supersonic jets were found to be similar to those of subsonic jets (rectangular—Krothapalli et al 1986; elliptic, rectangular, square, and triangular—Gutmark et al 1989b, 1991; rhombus—Alvi et al 1996). The noncircular jets had larger spreading rates compared to jets with circular geometry, especially at the jet sections with the larger radius of curvature (i.e. minor axis plane in an elliptical jet). This enhanced mixing resulted in accelerated decay of the mean velocity along the jet axis. The improved mixing was more pronounced in the off-design conditions of supersonic jet flow due to the interaction of the expansion/compression waves with the jet shear layer. The enhanced spreading rate at the minor axis plane was also accompanied by higher sound emission at this section of the jet. The spreading rate of the rectangular jet was somewhat lower than that of the elliptic jet, because its vertices reduced the coherence of the large-scale structures. The self-induction of these vortices, which led to the enhanced mixing rates, was therefore weakened. The sonic rectangular jet operating at design conditions was predominantly symmetric in both major and minor planes. At slightly underexpanded conditions, an asymmetric flapping mode appeared at the minor axis plane, resulting in a large spreading rate, whereas the major axis remained

symmetric with a small spreading rate. The characteristic nondimensional frequency associated with these vortices was $St_D = 0.12$. The large amplitude flapping was reduced at a higher M, and the jet became quasi-axisymmetric with large spreading rate at both axis planes. Schadow et al (1989) showed that the spatial growth rate of elliptic jets diminishes with increasing M. However, when the compressible jet eccentricity was varied from a circular jet to an elliptic jet with different AR, the growth rate and the phase velocity of the amplified waves were also changed.

Tam (1988) proposed a vortex sheet model to estimate the shock-cell structure of rectangular and other noncircular jets. He obtained good agreement with experimental data in predicting the shock-cell spacing and the screech frequency for large-AR jets in a range of sonic speed to $M = 2$. He predicted that the shock-cell spacing is directly proportional to M, while the screech-tone nondimensional frequency is inversely proportional to M.

The superior mixing characteristics of the underexpanded rectangular and elliptic free jets were also demonstrated in hot-flow experiments ($T = 1600K$). The large spreading rate of the elliptic jet at the minor axis plane compared to the major axis plane was measured in a supersonic elliptic reacting jet (Schadow et al 1989). The centerline temperature decay in the free-jet plume was faster in rectangular jets compared to an elliptic jet, and both showed lower centerline temperature than the circular jet (Gutmark et al 1989b). These results indicate that, unlike the nonreacting jet, the rectangular reacting jet has superior mixing characteristics compared with the elliptic reacting jet.

Axial vorticity generators such as tabs, vortex generators, and lobes were investigated as mixing promoters in supersonic flows. The streamwise vortices are located on the surface of underexpanded jets between the oblique shocks and the jet boundary. These vortices enhance the jet mixing with ambient fluid in the supersonic section. Novopashin & Perepelkin (1989) showed that these vortices are induced by small imperfections inside the nozzle, and thus it was reasonable to use larger vortex-producing devices such as vortex generators or tabs as mixing enhancers in supersonic jets.

Ahuja & Brown (1989) used tabs to enhance mixing and reduce screech noise in supersonic jets. The delta-shaped tabs produced a pair of counter-rotating vortices which improved mixing in the shear layer of sonic and supersonic underexpanded jets (Samimy et al 1993, Zaman et al 1994). A pair of tabs bifurcated the jet, and a larger number of tabs distorted the cross-section of the jet. Reeder & Samimy (1996) discussed the effect of the pair of counter-rotating, streamwise vortices generated by the tabs on the mixing enhancement observed in the jet. Although subharmonic axial forcing and tabs can independently increase jet spreading, a combination of both reduces the effect—due to the conflicting dynamics (with regard to jet spreading) of the excitation-induced

azimuthal vortices and the streamwise vortices induced by the presence of the tabs (Zaman & Raman 1997).

The effect of tabs was also investigated by Zaman (1994) in conjunction with noncircular geometries involving rectangular nozzles with various AR (3:1 to 8:1) and elliptic jets. The axis-switching phenomenon typical of elongated jets was controlled by the tabs and in some cases was suppressed, resulting in a change in the near-field rate of entrainment of the jet. The far-field ($x/D > 10$) spreading rates were mostly unaffected by the tabs. The mixing enhancement of the underexpanded supersonic jets was partially due to the interaction of the jet flow with the shocks produced by the tabs (Wishart et al 1993). Vortex generators enhanced mass entrainment characteristics of rectangular jets (Rogers & Parekh 1994). The vortex generators provided an efficient way to introduce axial vorticity into the jet at the proper location and with the desired vorticity strength and orientation. A co-rotating vortex pair yielded up to 50% increased entrained mass without adding to the noise generation (Surks et al 1994). Rectangular jets with a modified long side were used to generate streamwise vortices in order to enhance mixing and reduce noise (Samimy et al 1997). The nozzles performed well at underexpanded conditions but showed reduced performance or no change at design or overexpanded conditions.

Lobed mixers were shown to be effective in mixing supersonic flows by inducing strong axial vorticity while maintaining thrust level comparable to that of an axisymmetric nozzle. McVey & Kennedy (1989) used a lobed splitter plate to introduce axial vorticity into the mixing layer in order to enhance mixing and combustion efficiency at subsonic speeds. They pointed out the importance of enhancing the mixing of the primary and secondary streams at the molecular level while retaining the large-scale benefits accrued by the introduction of streamwise vorticity. Based on these two-dimensional mixing-layer tests, Tillman et al (1991) compared the mixing characteristics of splayed and saw-toothed jets with circular and rectangular jets having the same area, area ratio, and width. The $M = 1.5$ jets at a temperature of 1000°F discharged into a free stream flowing at $M = 0.5$. The splayed jet induced strong circulation and produced radial velocities without associated flow separations and pressure losses. The jet improved mixing and reduced the potential core length by a factor of two relative to a rectangular nozzle ($AR = 3.7$) operating at the same conditions. Tillman & Presz (1993) used this nozzle and obtained a sustained augmentation of the gross thrust in a mixer ejector configuration.

Axial vorticity generators in the shape of ramped fuel injectors were proposed to improve mixing in supersonic combustion applications in which parallel fuel injection was preferred. Northam et al (1989) investigated several geometries for the ramped fuel injectors and showed that swept ramps can yield higher combustion efficiency compared to unswept ones. The concept was extended

to supersonic flows by Yu et al (1992). A converging-diverging $M = 3$ nozzle having five axial vorticity producing swept ramps in its diverging section was tested. The shear layers of the ramped jets had significantly higher growth rates compared to those of a circular jet. The ramped injector was used in a supersonic combustion test in which high-temperature combustion products with excess hydrogen were discharged through the nozzle into a co-axial air stream. The radiation intensity at the near field of the ramped nozzle was much higher than in the circular nozzle, indicative of higher heat release relative to the circular injector.

Various other nonaxisymmetric supersonic convergent nozzles were tested in a fully expanded Mach number range of up to $M = 1.6$ (Wlezien & Kibens 1988). Asymmetric nozzles with either one short-extension tab or moderate inclination (beveling) generated deflection of the flow without significant change in the spreading rate. Nozzles with long-extension tabs, steep inclination, or with two extension tabs produced large spreading rate in one direction and contraction in the other. Beveled $M = 1.4$ converging/diverging and converging rectangular nozzles were compared with regular rectangular jets (Rice & Raman 1993). Single beveled jets showed marginal increase in spreading rate. Double beveling increased the jet entrainment rate by over 50% in the first 10 equivalent diameters. The double-beveled jet exhibited rapid transverse flow divergence, leading to bifurcation, and maintained axial flow to maximize thrust. Supersonic jets from notched nozzles were modified by the trailing vortices shed from the swept edges of the notches (Pannu & Johannesen 1976). The effect of these vortices was to enhance the jet spreading in the notch plane by forming low-speed side jets. The centerline decay rate was significantly enhanced. Jet noise was suppressed because the noise sources were surrounded by low-speed turbulent flow.

PHYSICAL MECHANISMS

Theoretical studies provided insight regarding initial conditions that promote the kind of azimuthally nonuniform growth behavior underlying the characteristic axis switching of noncircular jets. Studies of the stability of elliptic jets were reported by Crighton (1973) based on vortex sheet models and by Morris (1988) using more realistic finite-thickness shear layers. Koshigoe & Tubis (1986, 1987), Koshigoe et al (1989), and Baty & Morris (1989) presented frameworks for the study of the instability characteristics of jets with general shape. More recent stability studies of noncircular jets have focused on rectangular (Tam & Thiess 1993) and elliptical (Huang et al 1994, Morris & Bhat 1995) configurations. Time-dependent numerical simulations of noncircular jets investigated axis-switching and entrainment properties (Kiya et al 1992,

Grinstein 1993, Huang et al 1994, Grinstein et al 1995, Miller et al 1995), and associated underlying vortex dynamics (Grinstein 1995, Grinstein & DeVore 1996).

Jet Stability Characteristics

Based on linear stability analysis, Koshigoe et al (1988, 1989) proposed three requirements necessary to initiate the deformation of the noncircular vortex rings in a jet. The first requirement is that the eigenfunctions of the unstable modes should be localized within the jet circumference without excessive overlapping. The asymmetric shape of the nozzle, with circumferentially varying curvature, causes separation of the different instability modes and localizes the amplification at specific segments along the circumference (e.g. one mode is dominant at the major axis, whereas another mode is dominant at the minor axis of an elliptic jet). Second, the amplification rates of the corresponding eigenmodes should be comparable. This requirement can be fulfilled if the azimuthal nonuniformities of the initial shear layer are relatively small, so that the growth rates of the velocity fluctuations associated with the different modes are comparable. Third, sufficient phase-speed differences should exist between eigenmodes, so that the streamwise location where the vortex roll-up is completed relative to the edge of the nozzle is dependent on the azimuthal vortex-shedding location. For example, the vortex shed from the major-axis side of an elliptic nozzle completes its roll-up farther downstream relative to the vortex shed from the minor-axis side, the initial vortex deforms, and thus the axis-switching sequence is initiated (Figure 9). The fulfillment of these conditions depends on the initial azimuthal distribution of the momentum thickness and on the particular geometry of the nozzle.

Axis Switching and Initial Conditions

The occurrence of axis switching for a given noncircular nozzle geometry depends on initial conditions such as azimuthal distribution of momentum thickness θ, ratio D_e/θ, turbulence level, and jet forcing (Hussain & Husain 1989, Grinstein et al 1995). Nonuniform initial shear-layer thickness, in particular, has a significant impact on the number of observed axis switchings. For example, nonuniform θ in pipe nozzles—typically involving much thicker initial θ than orifice nozzles and relatively larger θ in the high curvature (e.g. corner) regions—has the clear effect of inhibiting axis switchings. In laboratory experiments with elliptic jets, a 3:1 jet issuing from a pipe did not show any axis switching (Schadow et al 1987b), with similar jet growth rates at the minor and major axis, both larger than for the round jet. This behavior was in contrast with that of the contoured elliptic jet (Ho & Gutmark 1987), which switched axes near the nozzle due to high spreading rate at the minor axis and nearly zero-growth at

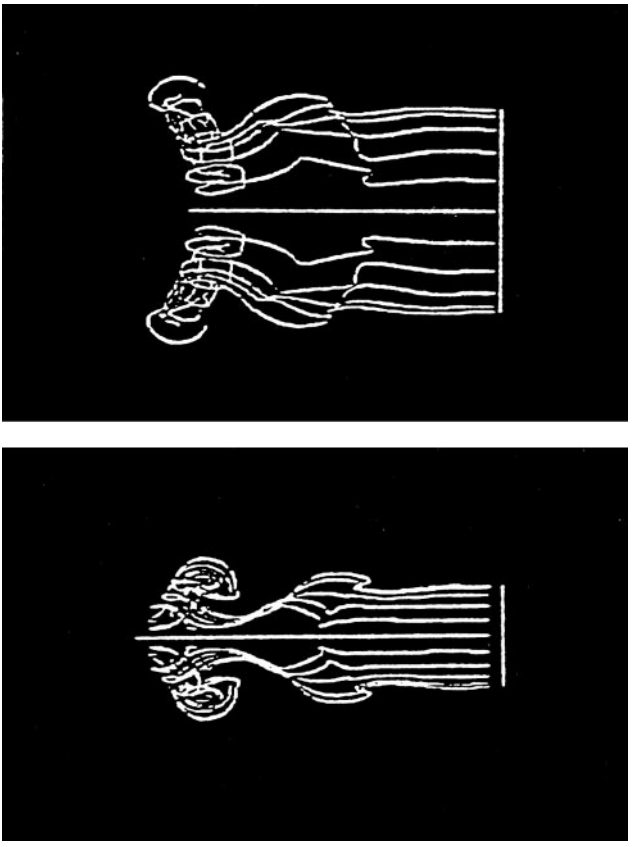

Figure 9 Streaklines of 2:1 elliptic jet projected onto the major (*a*) and minor (*b*) axis planes. (Huang et al 1994)

the major axis. Similar results were obtained when comparing pipe and orifice triangular (Koshigoe et al 1989) and square (Grinstein et al 1995) jets. The shear-layer growth rate at the vertex and flat sides of the pipe jets were similar, resulting in conservation of the initial triangular (or square) nozzle orientation of the jet cross-sections. However, the flat side grew faster than the vertex side in the orifice jet, resulting in a reversal (or 45-deg rotation) of the jet cross-section orientation at a distance of one nozzle diameter from the nozzle exit.

The axis-switching–inhibiting feature observed for pipe nozzle jets can also be attributed to secondary flows that are induced within ducts with corners (e.g. Su & Friedrich 1994). These secondary flows are characteristically directed away from the jet axis and toward the corners, thus leading to jet-width growth

at the jet exit in corner directions opposing the jet-width reduction accompanying the initial bending of the corner sections in the orifice jets. Axial forcing imposed at the jet exit can overcome the latter effect (Grinstein et al 1995) by enhancing the vortex ring strength and coherence, and thus the importance of the vortex ring self-deformation process. Behavior promoting axis switching can be found in nozzles with contraction conditions upstream for which secondary flows toward the jet axis are induced within the nozzle along the corners (e.g. Quinn 1992a). In addition, the flow induced by pairs of streamwise vortices generated by tabs placed at the edge of rectangular nozzles can effectively resist or enhance axis switching (Zaman 1996b), depending on their relative distribution at the rim of the nozzle (as shown in Figure 10). Thus, the interaction between the vortex ring dynamics and the initial streamwise vorticity can have a considerable role in affecting axis-switching phenomena.

Even if effectively absent at the jet exit, the streamwise vorticity dynamics has an increasingly more important role on the jet development in the downstream direction. In contrast with the plane free mixing layer, where two-dimensional spanwise vortex rollers are continuously supported by the imposed constant downstream shear, the velocity between the high-speed jet core and its surroundings decreases toward the end of the jet potential core, thus attenuating the shear supporting the vortex rings in the jet. Sufficiently far downstream, the dynamics of jets with moderate-to-high Re and high M is inherently three-dimensional, and the streamwise vorticity dominates entrainment (Liepmann & Gharib 1992).

Vortex Ring Dynamics

In the early views of axis switching (Abramovich 1983, Toyoda & Hussain 1989), the dynamics of vortex rings were presumed to dominate the jet development. Axis switchings of the jet cross-section were directly associated with successive self-induced axis rotations of vortex rings, and the important role of jet initial conditions and braid vortices was not recognized.

Based on theoretical (incompressible flow) analysis, Abramovich (1983) argued that successive axis switchings in rectangular jets could be explained by pressure differentials between vortex ring sections. In this picture of the jet cross-section deformation, differing effective shear-layer growths along major and minor jet axis directions play the main role in the axis-switching process. This is consistent with the stability analysis of Tam & Thiess (1993) indicating

Figure 10 Streamwise variation of rectangular jet half-width at the major and minor axis planes. (*a*) no tabs, (*b*) two tabs at narrow section, (*c*) two tabs at wide section, (*d*) with acoustic excitation. (Zaman 1996b)

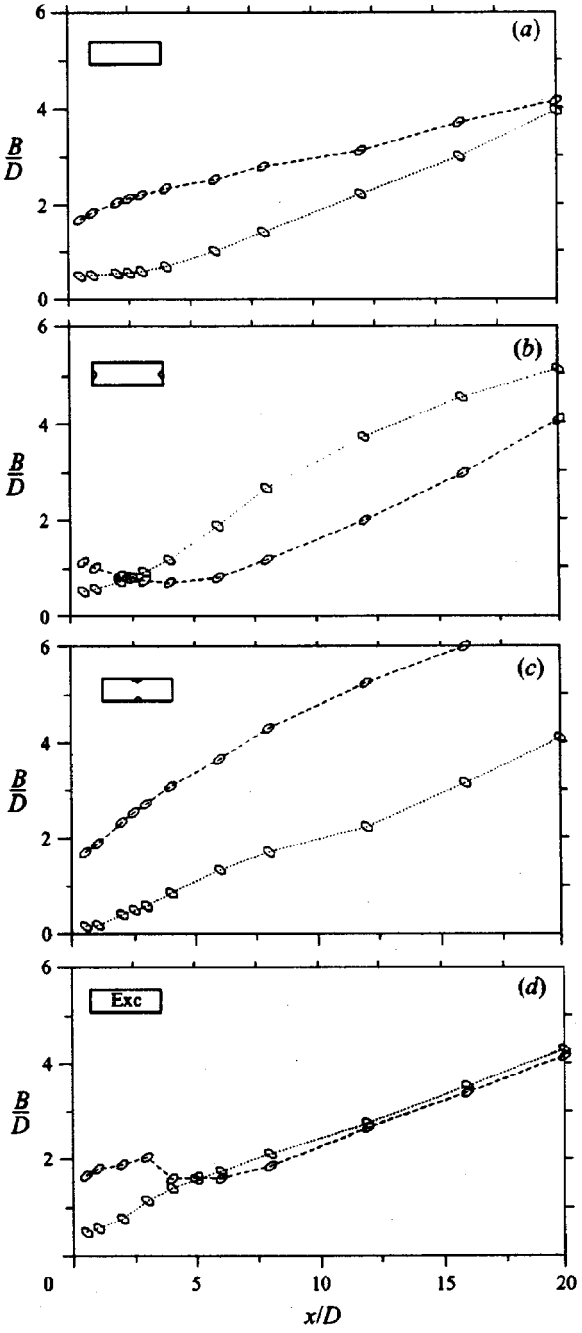
(a)
(b)
(c)
(d)
Exc
B/D
x/D
0
2
4
6
0
5
10
15
20

that the instability modes with faster spatial growth rates are those associated with pressure-fluctuation maxima localized near the centers of the sides of the rectangular shear layer.

Unlike the case of circular jets (Martin & Meiburg 1991, Lasheras et al 1991, Grinstein et al 1996), vortex ring deformation can occur in noncircular jets without the aid of azimuthal forcing. This is a result of Biot-Savart self-induction associated with azimuthal nonuniform shear-layer curvature. Such self-induced deformation was observed in the early laboratory experiments investigating the evolution of noncircular vortex rings (e.g. Kambe & Takao 1971, Oshima 1972, Viets & Sforza 1972). It is clearly distinct from vortex ring distortion due to azimuthal instabilities (Widnall & Sullivan 1973), which also affect the noncircular ring dynamics. Assuming incompressible and inviscid flow conditions, and modeling the vortex ring in terms of a thin vortex tube, the azimuthal variation of the self-induced velocity u responsible for the vortex-ring deformations was described by Batchelor (1967) as

$$u \sim C\,\mathbf{b}\log(1/\sigma), \tag{1}$$

where C is the local curvature of the tube, σ is its local cross-section, and **b** is the binormal to the plane containing the tube. Equation 1 predicts that, in the absence of azimuthal perturbations, a perfectly round, uniform ring will be convected without changes in shape and can also be used to explain successive self-induced axis rotations of an isolated vortex ring.

The development in space and time of isolated low-AR pseudo-elliptic (Kiya et al 1992) and rectangular (Grinstein 1995) vortex rings was investigated as a function of AR in computational studies. In these studies, by design, the self-induced ring dynamics was isolated from interactions with other CS otherwise present upstream and downstream of the rings in developed jets, from possible effects of azimuthal nonuniformities of the momentum thickness, and from presence of streamwise vorticity at the jet exit. The simulations showed that an isolated vortex ring undergoes quite regular self-induced nonplanar deformations for AR < 4, approximately recovering shape and flatness with axis rotated with respect to its initial configuration, and with axis-rotation periods exhibiting nearly linear proportionality to AR. Vortex ring splitting was observed for $12 \geq \text{AR} \geq 4$. The vortex reconnection dynamics underlying the vortex bifurcation process observed in the laboratory investigations (Hussain & Husain 1989, Toyoda & Hussain 1989) was demonstrated by Grinstein (1995) for vortex rings with AR $= 4$ (Figures 11 and 12).

Role of Braid Vortices

The dynamics of nonisolated vortex rings in developed jets can be significantly different from that of isolated rings, as the vortices move downstream away

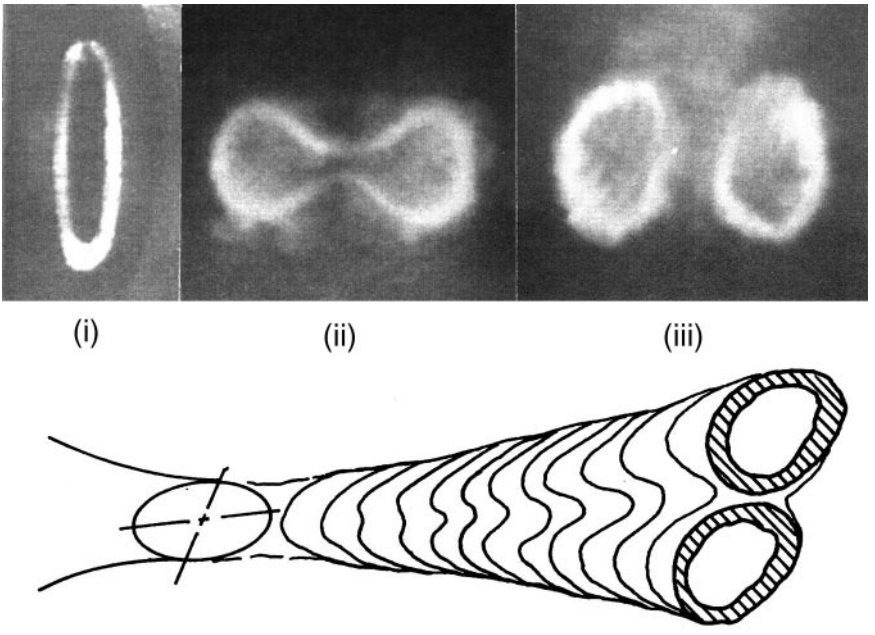

Figure 11 Vortex-ring bifurcation phenomena for elliptic AR = 4 jets. (i), (ii), and (iii) denote three successive phases of bifurcation at successive streamwise locations. (Hussain & Husain 1989)

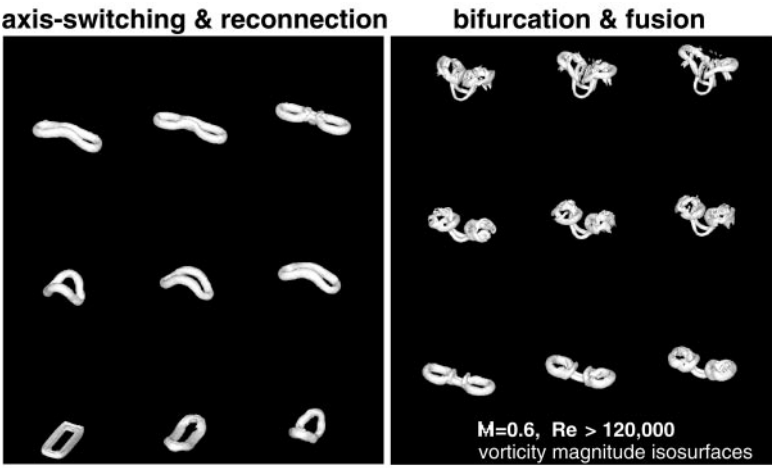

Figure 12 Vortex-ring bifurcation phenomena for rectangular AR = 4 jets. (Grinstein 1995)

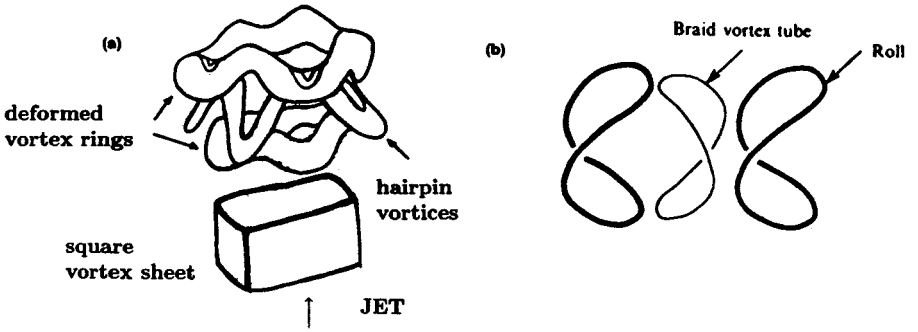

Figure 13 Geometries of interacting ring and braid vortices. a) square, AR = 1 (Grinstein & DeVore 1996), b) elliptic, AR = 2 (Husain & Hussain 1993)

from the jet exit and strong interactions with other large-scale vortices occur. In particular, the important role of interactions with streamwise braid vortices was recognized only recently. Braid (rib) vortices were identified in studies of square jets (Grinstein & DeVore 1992) and elliptic jets (Husain & Hussain 1993), where they were shown to appear as a result of redistribution and stretching of the streamwise vorticity in the braid regions between vortex rings. The characteristic coupling geometries of interacting braid and ring vortices for square (AR = 1) and elliptic (AR = 2) jets are compared in Figure 13. The braid-vortex generation mechanism involves distortion of the braid vortex loops induced by the deformation of neighboring vortex rings, which in the absence of streamwise vorticity at the jet exit plane, precedes the formation of the braid vortices in noncircular jets. This deformation is followed by vorticity concentration and stretching of these loops into vortices aligned with fixed azimuthal locations (e.g. corner regions) characteristic to the geometry at the jet exit. In addition to enhancing fluid entrainment from the jet surroundings, braid vortices induce further vortex ring deformation, trigger azimuthal instabilities, and have a direct role in affecting axis switching and the transition to turbulence. Farther downstream, strong interactions between ring and braid vortices lead to their breakdown as they become more contorted and incoherent, and a more disorganized regime dominated by smaller-scale, elongated vortices characterizes the jet flow (Grinstein & DeVore 1996).

Results of experiments, stability analysis, and simulations support the concept that the basic mechanism for the first axis rotation of the jet cross-section is the self-deformation of the vortex rings due to nonuniform azimuthal curvature at the initial jet shear layer. However, subsequent axis rotations of the jet cross-section are not necessarily linked to successive vortex-ring axis rotations.

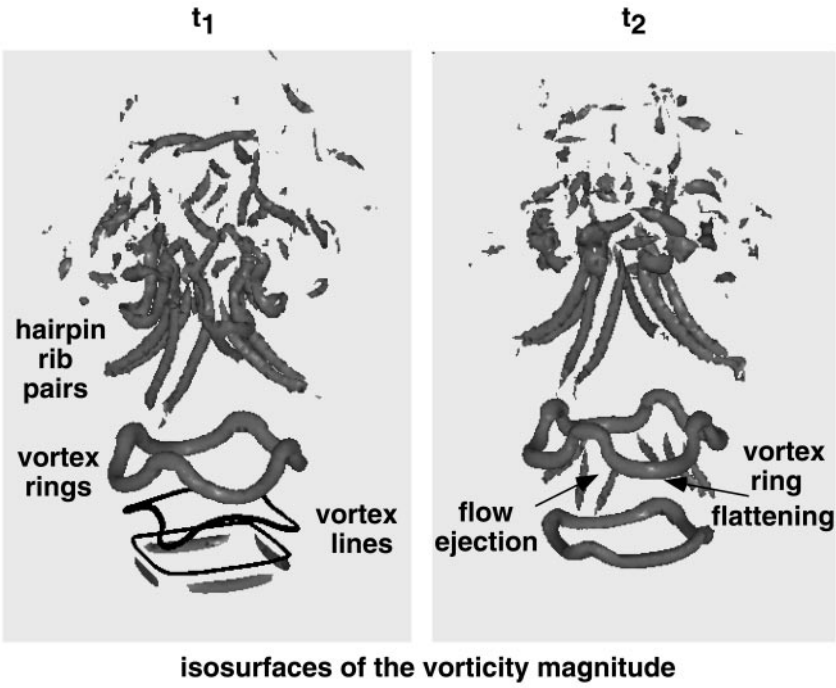

Figure 14 Interacting ring and braid vortices for low-AR rectangular free jets with AR = 1. Instantaneous visualizations at two consecutive times based on vorticity isosurfaces and vortex lines. (Grinstein & DeVore 1996)

Strong interactions with braid vortices and other rings can inhibit axis rotations of nonisolated rings, which do not recover shape and flatness after the initial self-deformation.

In the square jet case (Grinstein & DeVore 1996), for example, braid (hairpin) vortices induce flow ejection at the corner regions and flattening of the ring portions left behind after the initial ring self-deformation (Figure 14), and this mechanism leads to the second axis rotation of the jet cross-section. This is in contrast with the self-induced axis-rotation dynamics of isolated rings, a process in which ring shape and flatness are approximately recovered. In terms of jet spreading along characteristic directions, axis rotations first require faster growth on the flat sides (s-direction) and shrinking along the vertex direction (d-direction) so that crossover of jet widths along 's' and 'd' is possible. The self-distortion of the corner regions of the vortex ring is the mechanism underlying the initial shrinking along 'd,' depending directly on the local azimuthal curvature C and thickness σ (according to Equation 1). The dependence of

vortex-ring self-deformation effects on C, as implied by Equation 1, is qualitatively consistent with the analysis of stability theory (Koshigoe et al 1989), in spite of the limited (linear) nature of the latter analysis. Stability theory predicts that sections with large curvature have higher phase-speed, resulting in deformation of these vortex sections toward the downstream direction, consistent with the predictions of Equation 1. Linear stability theory does not, however, predict the effect of the local vortex thickness σ. After the first crossover of the characteristic jet widths, a new axis rotation will require, in turn, faster growth along 'd' so that a new crossover can occur. Depending on the particular jet initial conditions, several or no axis rotations can occur in the first few diameters of jet development. The eventual faster jet spreading along 'd' necessary to have a second crossover (and then a new axis rotation of the jet cross-section) is directly related to the strength of the hairpin vortices, inducing flow ejection at corner regions and flattening on the upstream portions of the undulating vortex rings.

Aspect-Ratio Effects

Laboratory investigations of rectangular (Tsuchiya et al 1986) and elliptic (Husain & Hussain 1983, Ho & Gutmark 1987) jets with AR ≥ 2 indicate that the spreading of the jet in the direction of the flow is accompanied by deformation of its transverse section. As the minor-axis side increases and the major-axis side decreases, the jet cross-section approaches an approximately rhomboidal-shape, and then, with subsequent development, the minor and major axis directions interchange, thus undergoing a 90-deg axis rotation (Figure 4). The unsteady jet vorticity dynamics for AR $= 3$ is illustrated in Figure 15 (see color section). As in the isolated ring case (cf Figure 12), in the first phase of the rectangular ring deformation, its corner regions move ahead faster due to the self-induced velocity; the higher-curvature portions left behind (at major-axis locations) then move faster ahead, and further self-induced deformation of the ring follows, where the minor sides of the ring stretch and effectively move faster downstream, while the centers of the longer sides tend to stay behind and move away from the jet centerline. However, rather than having the ring recover its approximate flatness and shape, this leads to a nonplanar vortex ring having a transverse cross-section with formally switched axes (relative to the jet exit). As noted above for AR $= 1$, the dynamical mechanisms underlying axis switchings, subsequent to the first, cannot be attributed to just vortex-ring self-deformation. In the downstream direction, the jet development is controlled by strong interactions between ring and braid vortices, which combined with azimuthal instabilities, will eventually lead to their breakdown and to the more disorganized (turbulent) flow regime downstream.

After the corner regions of the rectangular rings become effectively rounded in the early vortex-ring deformation phase, their dynamics is essentially

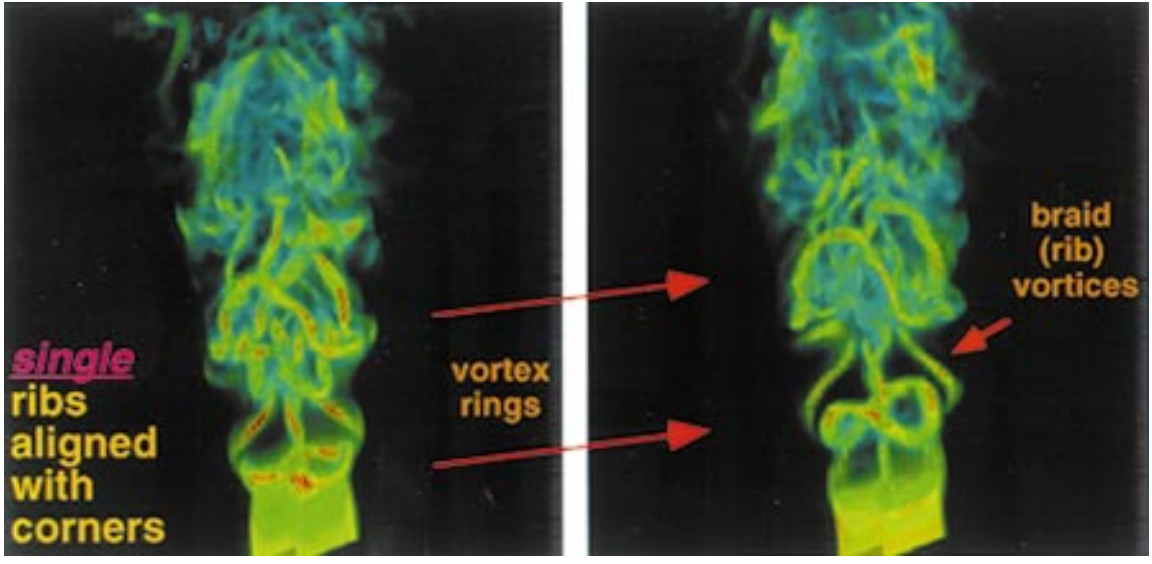

Figure 15 Instantaneous volume visualization of the vorticity magnitude for a rectangular free jet with AR = 3 (Grinstein 1998).

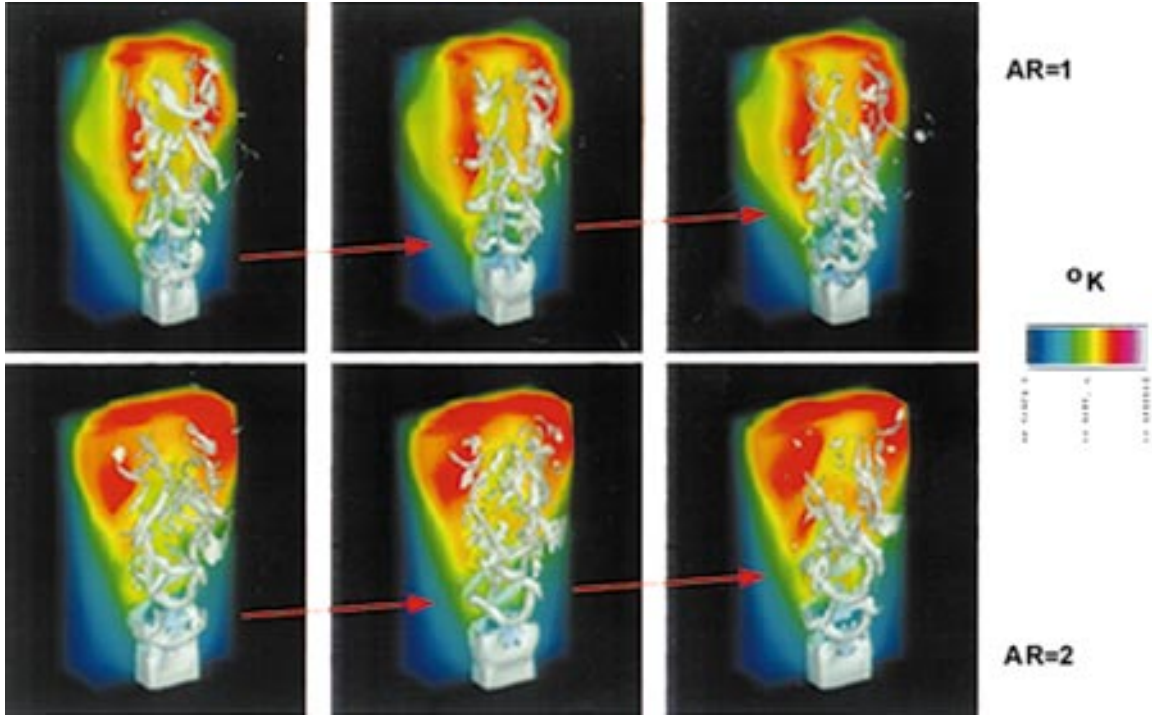

Figure 16 (opposite) Instantaneous temperature distributions superimposed on isosurfaces of the vorticity magnitude (50% peak value) for AR = 1 (top) and AR = 2 (bottom). Grinstein (1998).

equivalent to pseudo-elliptic (Kiya et al 1992) and elliptic (Hussain & Husain 1989) rings with the same AR. Thus, the two qualitatively different rib-ring coupling geometries, shown in Figure 13, are also representative for rectangular jets in general, and rectangular jets with AR ≥ 2 are characterized by single ribs aligned with corner regions, in contrast with pairs of counter-rotating ribs aligned with the corners for square jets (Figure 14). The jet vorticity dynamics will present further distinct topological features for larger AR (e.g. for AR ≥ 4), for which vortex ring bifurcation (Figures 11 and 12) has been observed (Toyoda & Hussain 1989, Hussain & Husain 1989, Kiya et al 1992, Grinstein 1995).

The database of jet simulations can also be used to obtain insights on the close relationship between unsteady fluid and combustion dynamics of a fuel jet emerging into an oxidizer background (Grinstein & Kailasanath 1995, 1996), and in particular, to assess the potential impact of AR on non-premixed rectangular jet combustion (Grinstein 1997). This is illustrated in Figure 16 (see color section), where typical instantaneous jet visualizations for jets with AR $= 1$ and AR $= 2$ are shown. By design, the jet cases compared, differ on the actual shape of the initial jet cross-section but have otherwise identical initial conditions, e.g. including the same cross-sectional jet outlet areas. The near-jet entrainment and non-premixed combustion properties of the low-AR rectangular jets are largely determined by the characteristic braid-vortex topology and vortex-ring axis-rotation times. Because of the initial enhanced entrainment associated with rib pairs aligned with the corner regions, the square jet combustion is more effective immediately downstream of the nozzle. On the other hand, the jet with AR $= 2$ exhibits better combustion farther away from the jet exit, reflecting better entrainment there due to azimuthally stable vortex rings and the axis-switching process being completed farther downstream, since vortex-ring axis-rotation times increase with AR (Kiya et al 1992, Grinstein 1995). An important open question relates to whether an optimal AR exists with regard to entrainment enhancement. Laboratory jet experiments with pseudo-elliptical geometries (Schadow et al 1987a) suggest that an optimal AR with regard to nozzle-geometry–enhanced entrainment might be at a value AR $= 3$. However, the experiments are not conclusive since the studies involved AR up to 3.5 and nonuniform momentum thickness distributions—which are known to also affect the entrainment process (Koshigoe et al 1989, Hussain & Husain 1989). For AR > 3.5, the important effects on jet entrainment of other more complicated interactions, such as vortex ring bifurcation, have been demonstrated (Hussain & Husain 1989).

APPLICATIONS

Understanding the detailed dynamics of jet entrainment and mixing is of fundamental importance to various applications such as noise suppression,

combustion, lift augmentation, heat transfer, and chemical reactors. Noncircular jets were used to improve performance of various types of airbreathing engines and other combustors, to obtain thrust vector control (TVC), to abate jet noise, and to enhance supersonic mixing.

Jet Noise

Ahuja et al (1990) compared several nozzle geometries to evaluate their effect on jet noise reduction in high-subsonic and supersonic jets. He concluded that the circular jet produces the highest level of noise. The noise produced by rectangular jets was lower compared to that of the circular jet, with a higher level emitted at the wider side. Reductions were obtained in both subsonic and supersonic velocities. Triangular jets yielded similar reductions, particularly at the directions aligned with their bases. The elliptic jets showed a small noise reduction at subsonic speeds but a small increase in both axes at a supersonic speed. Adding tabs to the circular or rectangular nozzles was found to be ineffective, and actually increased the broadband noise, especially at subsonic speeds. Adding two notches to the circular jet and the rectangular jet was ineffective, but four notches in the rectangular jet reduced the noise in the major axis plane. All these observations were related to the effects of the various nozzle configurations on the jet-mixing rate.

Heat Transfer

An impinging elliptic jet with AR ≈ 2 was used to augment heat transfer between the jet and a flat plate. The maximum heat transfer at the stagnation point for the elliptic jet occurred at a shorter nozzle-to-plate distance compared to a circular jet due to the shorter length of the elliptic jet potential core. The Nusselt number in the impingement region for the elliptic jet was larger than that of the circular jet due to the larger entrainment and the dynamics of the large-scale coherent structures (Lee et al 1994).

Combustion and Mixing Control

Understanding the detailed dynamics of jet entrainment and mixing is of fundamental importance for achieving efficient and environmentally clean combustion. The mixing between the reactants in diffusion flames, or between the hot reaction products and the fresh reactants needed to sustain combustion, is a crucial part of the combustion process. The mixing occurs in two stages. The initial stage brings relatively large amounts of the reactants together (large-scale stirring) and is associated with the entrainment process through vortex dynamics. The second stage involves small-scale turbulent mixing, which accelerates the molecular contact between the reactants. Noncircular jets can be used to enhance both the large-scale and small-scale mixing necessary for efficient combustion. Some investigations that demonstrated the use of noncircular jets

for augmented energy release, reduced emissions, and combustion stabilization were discussed in previous sections of this review.

Thrust Vector Control (TVC)

Aerodynamic TVC methods have the potential to be simpler than mechanical means with lower weight penalty, thrust loss, and cost. Elongated jets, such as rectangular, elliptic, or diamond shaped, are better suited for aerodynamic-based control than are circular nozzles due to the inherent lateral instability in their wide dimension. An example of such an aerodynamic method is thrust redirection by counterflow, which was proposed as a means of TVC and is more easily applicable in noncircular configurations (Strykowski et al 1996).

SUMMARY

This review discussed the flow field of several different noncircular jet geometries and the pertinent physical mechanisms that control their development. The geometrical configurations considered included the effects of (*a*) nozzle eccentricity in elliptic and rectangular jets, (*b*) sharp corners in rectangular and triangular jets, and (*c*) axial vorticity generators at the jet exit in circular and noncircular nozzles. Several issues were common to all noncircular shapes; they included axis switching and the azimuthal variation of the shear-layer spreading rate and turbulence production.

The evolution of the jets was shown to depend strongly on initial conditions at the nozzle exit. It included parameters such as the initial azimuthal momentum-thickness distribution at the nozzle lip, the ratio of shear-layer-thickness to jet equivalent diameter, the local shear-layer curvature, the eccentricity measured by the nozzle geometrical aspect ratio, Reynolds and Mach numbers, and the jet-to-background velocity and density ratios. These initial conditions determine the structure of the asymmetric vortices that roll up in the near jet field. As the vortices convect downstream, vortex deformation and self-induction processes control the downstream evolution of the jet, leading under certain conditions to the axis-switching phenomenon. The increased entrainment characteristics and enhanced fine-scale mixing of noncircular jets are the result of complex interactions between azimuthal and streamwise vortices, which are unique to this type of flow field.

ACKNOWLEDGMENTS

This work was supported by the Mechanics and Energy Conversion Division of ONR, with Dr. Gabriel Roy as Scientific Officer. The DoD HPC-MP at CEWES provided computer time.

Literature Cited

Abramovich GN. 1983. Deformation of the transverse section of a rectangular turbulent jet. *Isz. Akad. Nauk. SSSR, Mekh. Zhidk. Gaza* 1:54–63

Ahuja KK, Brown WH. 1989. Shear flow control by mechanical tabs. *AIAA Pap. 89–0994*

Ahuja A, Manes J, Massey K. 1990. An evaluation of various concepts of reducing supersonic jet noise. *AIAA Pap. 90–3982*

Alvi F, Krothapalli A, Washington D, King C. 1996. Aeroacoustic properties of a supersonic diamond shaped jet. *AIAA J.* 34:1562–69

Austin T. 1992. The small scale topology of a 2:1 aspect-ratio elliptic jet. PhD thesis. Univ. South. Calif., Los Angeles

Batchelor GK. 1967. *An Introduction to Fluid Dynamics*, p. 510. Cambridge, UK: Cambridge Univ. Press

Baty RS, Morris PJ. 1989. Instability of jets of arbitrary geometry. *AIAA Pap. 89–1796*

Bernal L, Roshko A. 1986. Streamwise vortex structures in plane mixing layers. *J. Fluid Mech.* 170:499–525

Bogdanoff DW. 1982. Compressibility effects in turbulent shear layers. *AIAA J.* 21:926–27

Bradbury LJS, Khadem AH. 1975. The distortion of a jet by tabs. *J. Fluid Mech.* 70:801–13

Brown G, Roshko A. 1974. On density effects and large structure in turbulent mixing layers. *J. Fluid Mech.* 64:775

Crighton D. 1973. Instability of an elliptic jet. *J. Fluid Mech.* 59:665–72

Crow SC, Champagne FH. 1971. Orderly structure in jet turbulence. *J. Fluid Mech.* 48:547

Dhanak MR, Debernardinis B. 1981. The evolution of an elliptic vortex ring. *J. Fluid Mech.* 109:189

Gollahalli S, Khanna T, Prabhu N. 1992. Diffusion flames of gas jets issued from circular and elliptic nozzles. *Combust. Sci. Technol.* 86:267

Grinstein FF. 1993. Vorticity dynamics in spatially-developing rectangular jets. *AIAA Pap. 93–3286*

Grinstein FF. 1995. Self-induced vortex ring dynamics in subsonic rectangular jets. *Phys. Fluids* 7:2519

Grinstein FF. 1998. Vortex dynamics and transition to turbulence in rectangular free jets, submitted to *J. Fluid Mech*., See also *ASME FEDSM 98-5307*

Grinstein FF, DeVore CR. 1992. Coherent structure dynamics in spatially-developing square jets. *AIAA Pap. 92–3441*

Grinstein FF, DeVore CR. 1996. Dynamics of coherent structures and transition to turbulence in free square jets. *Phys. Fluids* 8:1237–51

Grinstein FF, Gutmark EJ, Parr T. 1995. Near-field dynamics of subsonic, free square jets. A computational and experimental study. *Phys. Fluids* 7:1483–97

Grinstein FF, Gutmark EJ, Parr TP, Hanson-Parr DM, Obeysekare U. 1996. Streamwise and spanwise vortex interaction in an axisymmetric jet. A computational and experimental study. *Phys. Fluids* 8:1515–24

Grinstein FF, Kailasanath K. 1995. Three-dimensional numerical simulations of unsteady reactive square jets. *Combust. Flame* 100:2–10, 101:192

Grinstein FF, Kailasanath K. 1996. Exothermicity and three-dimensional effects in unsteady propane square jets. *26th Symp. (Int.) Combust.*, pp. 91–96. Pittsburgh, PA: Combust. Inst.

Gutmark EJ, Schadow KC. 1987. Flow characteristics of orifice and tapered jets. *Phys. Fluids* 30:3448–54

Gutmark EJ, Schadow KC, Bicker C. 1990. Near acoustic field and shock structure of rectangular supersonic jets. *AIAA J.* 28:1163–70

Gutmark EJ, Schadow KC, Parr TP, Hanson-Parr DM, Wilson KJ. 1989a. Noncircular jets in combustion systems. *Exp. Fluids* 7:248

Gutmark EJ, Schadow KC, Wilson KJ. 1989b. Noncircular jet dynamics in supersonic combustion. *J. Propuls. Power* 5:529–33

Gutmark EJ, Schadow KC, Wilson KJ. 1991. Subsonic and supersonic combustion using noncircular injectors. *J. Propuls. Power* 7:240–49

Herzberg J, Ho CM. 1995. Three dimensional vortex dynamics in a rectangular sudden expansion. *J. Fluid Mech.* 289:1–27

Ho CM, Gutmark EJ. 1987. Vortex induction and mass entrainment in a small-aspect ratio elliptic jet. *J. Fluid Mech.* 179:383

Ho CM, Huerre P. 1984. Perturbed free shear layers. *Annu. Rev. Fluid Mech.* 16:365–424

Huang S, Brown E, Mutter T. 1994. A phenomenological study of jet mixing: insights from linear stability analysis. *AIAA Pap. 94–0704*

Husain HS, Hussain AKMF. 1983. Controlled excitation of elliptic jets. *Phys. Fluids* 26: 2763

Husain HS, Hussain AKMF. 1993. Elliptic jets. Part 3. Dynamics of preferred mode coherent structure. *J. Fluid Mech.* 248:315

Hussain AKMF. 1986. Coherent structures and turbulence. *J. Fluid Mech.* 173:303

Hussain AKMF, Husain HS. 1989. Elliptic jets. Part I. Characteristics of unexcited and excited jets. *J. Fluid Mech.* 208:257

Kambe T, Takao T. 1971. Motion of distorted vortex rings. *J. Phys. Soc. Japan* 31:591

Kiya M, Toyoda K, Ishii H, Kitamura M, Ohe T. 1992. Numerical simulation and flow visualization experiment on deformation of pseudo-elliptic vortex rings. *Fluid Dyn. Res.* 10:117

Kolluri P, Kamal A, Gollahalli S. 1996. Application of noncircular primary-air inlet geometries in the inshot burners of residential gas furnaces. *J. Energy Res. Tech.* 118:58

Koshigoe S, Gutmark EJ, Schadow KC. 1989. Initial development of non-circular jets leading to axis switching. *AIAA J.* 27:411

Koshigoe S, Tubis A. 1986. Wave structure in jets of arbitrary shape. I. Linear inviscid spatial instability analysis. *Phys. Fluids* 29:3982–93

Koshigoe S, Tubis A. 1987. Wave structure in jets of arbitrary shape. II. Application of a generalized shooting method to linear stability analysis. *Phys. Fluids* 29:1715–23

Koshigoe S, Gutmark EJ, Schadow KC, Tubis A. 1988. Wave structures in jets of arbitrary shape. III. Triangular jets. *Phys. Fluids* 3:1410–19

Krothapalli A, Hsia H, Baganoff D, Karamcheti K. 1986. The role of screech tones in mixing of an underexpanded rectangular jet. *J. Sound Vib.* 106:119–43

Lasheras JC, Lecuona A, Rodriguez P. 1991. Three-dimensional vorticity dynamics in the near field of co-flowing forced jets. *Lect. Appl. Math.* 28:403–22

Lee S, Lee J, Lee D. 1994. Local heat transfer measurements from an elliptic jet impinging on a flat plate using liquid crystal. *Int. J. Heat Mass Trans.* 37:967–76

Liepmann D, Gharib M. 1992. The role of streamwise vorticity in the near-field entrainment of round jets. *J. Fluid Mech.* 245:643–68

Liu H, Wu S. 1995. Enhanced mixing of 2D lobed nozzles. *Int. Gas Turbine Aeroengine Congr. ASME 95-GT–339*

Martin J, Meiburg E. 1991. Numerical investigation of three dimensionally evolving jets subject to axisymmetric and azimuthal perturbations. *J. Fluid Mech.* 230:271–318

McMurtry PA, Riley JJ, Metcalfe RW. 1989. Effects of heat release on the large-scale structure in turbulent mixing layers. *J. Fluid Mech.* 199:297–332

McVey J, Kennedy J. 1989. Flame propagation enhancement through streamwise vorticity stirring. *AIAA Pap. 89–0619*

Michalke A. 1971. Instability of a compressible circular free jet with consideration of the influence of the jet boundary layer thickness. *NASA TM 75190*

Miller RS, Madnia CK, Givi P. 1995. Numerical simulation of non-circular jets. *Comput. Fluids* 24:1–25

Monkewitz P, Pfizenmaier E. 1991. Mixing by side jets in strongly forced and self-excited round jets. *Phys. Fluids A* 3:1356–61

Morris PJ. 1988. Instability of elliptic jets. *AIAA J.* 26:172–78

Morris PJ, Bhat TRS. 1995. The spatial instability of compressible elliptic jets. *Phys. Fluids* 7:185–94

Northam B, Greenberg I, Byington C. 1989. Evaluation of parallel injector configurations for supersonic combustion. *AIAA Pap. 89–2525*

Novopashin SA, Perepelkin AL. 1989. Axial symmetry loss of a supersonic preturbulent jet. *Phys. Lett. A* 135:290–93

Oshima Y. 1972. Motion of vortex rings in water. *J. Phys. Soc. Japan* 32:1125

Pannu SS, Johannesen NH. 1976. The structure of jets from notched nozzles. *J. Fluid Mech.* 74:515–28

Paterson R. 1984. Turbofan mixer nozzle flow field– a benchmark experimental study. *J. Eng. Gas Turbines Power* 106:692–98

Quinn WR. 1989. On mixing in an elliptic turbulent free jet. *Phys. Fluids A* 1:1716–22

Quinn WR. 1992a. Streamwise evolution of a square jet cross-section. *AIAA J.* 30:2852

Quinn WR. 1992b. Turbulent free jet flows issuing from sharp-edged rectangular slots: the influence of slot aspect-ratio. *Exp. Therm. Fluid Sci.* 5:203–15

Reeder M, Samimy M. 1996. The evolution of a jet with vortex generating tabs: real time visualization and quantitative measurements. *J. Fluid Mech.* 311:73–118

Rice E, Raman G. 1993. Supersonic jets from beveled rectangular nozzles. *ASME Winter Annu. Mtg.*, New Orleans, LA

Rogers C, Parekh D. 1994. Mixing enhancement and noise reduction by streamwise vortices in an air jet. *AIAA J.* 32:464–71

Roshko A, Papamoschou D. 1986. Observation of supersonic free shear layers. *AIAA Pap. 86–0162*

Samimy M, Kim J, Clancy P. 1997. Supersonic jet noise reduction and mixing enhancement through nozzle trailing edge modifications. *AIAA Pap. 97–0146*

Samimy M, Zaman KBMQ, Reeder MF. 1993. Effect of tabs on the flow and noise field of an axisymmetric jet. *AIAA J.* 31:609–19

Schadow KC, Gutmark EJ. 1989. Review of passive shear-flow control research for improved subsonic and supersonic combustion. *AIAA Pap. 89–2786*

Schadow KC, Gutmark EJ, Parr DM, Wilson KJ. 1988. Selective control of flow coherence in triangular jets. *Exp. Fluids* 6:129–35

Schadow KC, Gutmark EJ, Wilson KJ, Parr D, Mahan V, Ferrell G. 1987a. Effect of shear-flow dynamics in combustion processes. *Combust. Sci. Technol.* 54:103

Schadow KC, Wilson KJ, Lee MJ, Gutmark EJ. 1987b. Enhancement of mixing in reacting fuel-rich plumes issued from elliptical jets. *J. Propuls. Power* 3:145

Schadow KC, Gutmark EJ, Wilson KJ, Smith R. 1990. Noncircular inlet duct cross-section to reduce combustion instabilities. *Combust. Sci. Technol.* 73:537

Sfeir AA. 1975. Three-dimensional turbulent jet. *Proc. Can. Congr. Appl. Mech., 5th*, pp. 445–46

Sfeir AA. 1976. The velocity and temperature fields of rectangular jets. *Int. J. Heat Mass Transf.* 19:1289–97

Sfeir AA. 1979. Investigation of three-dimensional turbulent rectangular jets. *AIAA J.* 17: 1055–60

Sforza PM, Steiger MH, Trentacoste N. 1966. Studies on three-dimensional viscous jets. *AIAA J.* 4:800

Shih C, Krothapalli A, Gogineni S. 1992. Experimental observations of instability modes in a rectangular jet. *AIAA J.* 30:2388–94

Strykowski P, Krothapalli A, Forliti DJ. 1996. Counterflow thrust vectoring of supersonic jets. *AIAA J.* 34:2306–14

Su MD, Friedrich R. 1994. Investigation of fully developed turbulent flow in a straight duct with large eddy simulation. *ASME J. Fluids Eng.* 116:677

Surks P, Rogers C, Parekh D. 1994. Entrainment and acoustic variations in a round jet from introduced streamwise vorticity. *AIAA J.* 32:2108–10

Tam CKW. 1988. The shock-cell structures and screech tone frequencies of rectangular and non-axisymmetric supersonic jets. *J. Sound Vib.* 121:135–47

Tam CKW, Thiess AT. 1993. Instability of rectangular jets. *J. Fluid Mech.* 248:425

Tillman T, Patrick WP, Paterson RW. 1991. Enhanced mixing of supersonic jets. *J. Prop. Power* 7:1006–14

Tillman T, Presz W. 1993. Thrust characteristics of a supersonic mixer ejector. *AIAA Pap. 93–4345*

Toyoda K, Hussain AKMF. 1989. Vortical structures of noncircular jets. *Proc. Asian Congr. Fluid Mech., 4th*, Hong Kong, pp. A117–27

Trentacoste N, Sforza PM. 1967. Further experimental results for three-dimensional free jets. *AIAA J.* 5:885

Tsuchiya Y, Horikoshi C, Sato T. 1986. On the spread of rectangular jets. *Exp. Fluids* 4:197–204

Vandsburger U, Ding C. 1995. The spatial modulation of a forced triangular jet. *Exp. Fluids* 18:239–48

Viets H, Sforza PM. Dynamics of bilaterally symmetric vortex rings. 1972. *Phys. Fluids* 15:230

Whitelaw J, Sivasegaram S, Schadow KC, Gutmark EJ. 1988. Oscillations in non-axisymmetric dump combustor. *AGARD-CPP–450, Pap. 15*

Widnall SE, Sullivan JP. 1973. On the stability of vortex rings. *Proc. R. Soc. London A.* 332:35

Wishart DP, Krothapalli A, Mungal MG. 1993. Supersonic jet control via point disturbances inside the nozzle. *AIAA J.* 31:1340–1

Wlezien RW, Kibens V. 1988. Influence of nozzle asymmetry on supersonic jets. *AIAA J.* 26:27–33

Yu K, Kraeutle KH, Wilson KJ, Parr TP, Smith RA. 1992. Supersonic flow mixing and combustion using ramp nozzle. *AIAA Pap. 92–3840*

Zaman KBMQ. 1986. Flow field and near and far sound field of a subsonic jet. *J. Sound Vib.* 106:1–16

Zaman KBMQ. 1991. Effects of tabs on the evolution of an axisymmetric jet. *NASA TM 104472*

Zaman KBMQ. 1994. Effect of 'delta tabs' on mixing and axis switching in jets from asymmetric nozzles. *AIAA Pap. 94–0186*

Zaman KBMQ. 1996a. Spreading characteristics and thrust of jets from asymmetric nozzles. *AIAA Pap. 96–0200*

Zaman KBMQ. 1996b. Axis switching and spreading of an asymmetric jet: the role of coherent structure dynamics. *J. Fluid Mech.* 316:1–27

Zaman KBMQ, Raman G. 1997. Reversal in spreading of a tabbed circular jet under controlled excitation. *Phys. Fluids* 9:3733–41

Zaman KBMQ, Reeder M, Samimy M. 1994. Control of an axisymmetric jet using vortex generators. *Phys. Fluids* 6:778–92